⟨Original⟩

An Experimental and Theoretical Evaluation
of the Axial Vibration Properties of a Typical Drillstring

드릴스트링의 종진동 특성에 대한

실험적 및 이론적 연구

Lee, Hyun Yup*

이　　현　　엽

ABSTRACT

An analytical model for drillstring axial vibration is proposed. The drillstring is modelled as an equivalent stepwise uniform bar, and the bottom boundary is modelled as a spring and a damper which depend on WOB(weight on bit). The effect of tool joints and the effect of surrounding layers, such as mud and formation, are evaluated theoretically. To investigate the bottom boundary condition, a forced axial vibration testing technique was developed and the tests with a typical drillstring were performed at various WOB's. The results show good agreement with theoretical results. An important conclusion is that the flexibility of the bottom rock must be included in order to predict resonant frequencies of the drillstring axial vibration.

요　　약

드릴스트링의 종진동 해석을 위한 이론적 모델을 제시하였다. 드릴스트링은 균일봉들로 모델링하였으며, 비트와 바닥 암석과의 경계조건은 스프링과 댐퍼로 모델링하였다. 연결부(tool joint)의 영향, 드릴스트링 주위의 진흙물(mud)과 주변암석의 영향등은 이론적으로 산정하였다. 비트에서의 경계조건을 산정하기 위하여, 드릴스트링의 종진동에 대한 강제진동시험기법을 개발하여 실제의 드릴스트링에 대한 실험을 비트에 걸리는 힘(WOB)을 변화시키면서 수행하였다. 그 결과는 이론치와 잘 일치함을 확인하였다. 본 연구 결과 가장 중요한 결론은 드릴스트링의 종진동해석에 있어서, 바닥 암석의 강성이 고려되어야 하며, 이 강성은 비트에 걸리는 힘의 크기에 따라 다르다는 것이다.

1. Introduction

Drillstring Axial vibration has received much attention in the literature[1~6]. However, in practice, many axial vibration phenomena observed in the field are more complex than can be explained by the existing analytical models. This is mainly due to lack of understanding the bit/formation interaction which forms the bottom boundary condition and excitation.

In this research, forced vibration tests without actual drilling were performed. A forced vibration testing technique was developed, which utilized the hydraulic ram as a source of oscillatory axial excitation. In these tests, there was no excitation from the

*Member, Hong Ik University

bit because the bit was off the bottom or was not rotating. Therefore, the measured vibrations can be assumed to come from the topside excitation only. These tests are relatively easy to analyze compared to actual drilling, because the only excitation force from the topside was directly measured.

The forced vibration test with the bit off the bottom revals good agreement with theoretical predictions for the drillstring with a free bottom boundary condition. The purpose of this off-bottom test was to have a benchmark response measurement at a known free boundary condition at the bit. Tests were also performed at various WOB's without rotation. The effect of WOB on the effective bottom boundary condition was investigated with help of theoretical analyses.

In the analytical model, the drillstring is modelled as a stepwise uniform bar with spring-damper bottom boundary condition. A computer code has been implemented to obtain transsfer functions, which are responses due to unit harmonic input excitation, for stepwise uniform bars with mass-spring-damper boundary conditions. The solution technique used in this code is the transfer matrix method[7,8], which is based on the computation of the mobilities of uniform bars and mass-spring-damper systems. The Green's function approach is used to obtain the mobilities of uniform bars.

In this paper, English units are adopted and the conversion factors for SI units are given in Table 1.

2. Description of Field Experiments and Topside Excitation

The field experiments were performed at a test well in Tulsa, Oklahoma, in March and April of 1989. The length of the drillstring was 1718 ft and the bottom formation was dolomite. Fig. 1 shows a schematic diagram of the drilling system of the test well.

The drillstring is assembled with 30.2 ft long sections of 4.6 inch aluminum pipe with steel tool joints, and with a BHA(bottom hole assembly) consisting of 30.5 ft long 6.5 inch steel drill collars, as shown in Fig. 1. In this drilling system, the drawworks uses a hydraulic ram to raise and lower the power swivel and the drillstring. The ram is connected to the power swivel through a system of cables and blocks in the derrick. The drilling system is described in

Table 1 Conversion factors for SI units

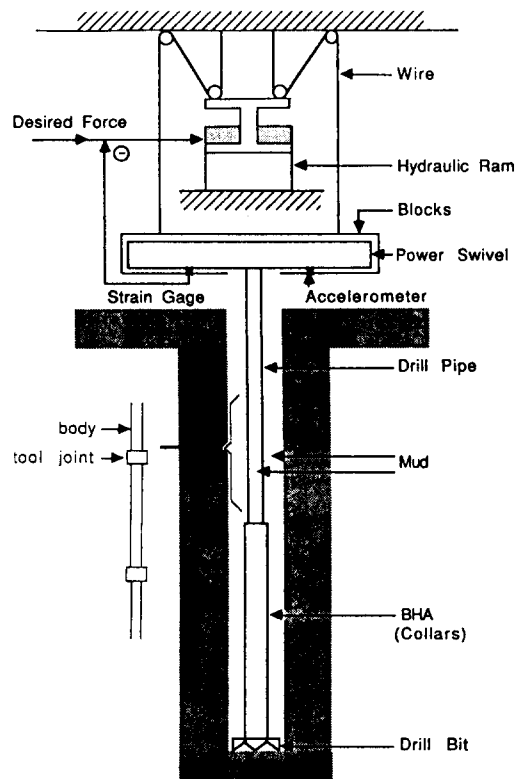| Quantity	English unit	SI unit
Length	1 ft	0.3048 m
	1 in	0.0254 m
Force	1lb	4.448 N
Mass	1slug	14.59 kg
Area	1ft^2	0.09290 m^2
Volume	1ft^3	0.02832 m^3
Pressure	1lb/ft^2	47.88 N/m^2
	1lb/in^2(psi)	6894 N/m^2
Density	1slug/ft^3	515.4 kg/m^3
Damping	1lb sec/ft	14.59 N sec/m
	1lb sec/ft^2	47.88 N sec/m^2
Viscosity	1lb sec/ft^2	47.88 N sec/m^2

Fig. 1 Schematic diagram of the drilling system in field experiments

Table 2, and the material properties used in the theoretical analyses are given in Table 3.

A forced vibration testing technique was developed, which utilized the hydraulic ram as a source of oscillatory axial excitation. The hydraulic ram lowers or raises the drillstring in response to a feedback control system, as shown in Fig. 1. Dynamic excitation to the drillstring was provided by using a signal from a signal generator as the ram control signal instead of the feedback control system. The excitation signal was band limited random noise with a frequency band of $0 \sim 20$ Hz.

As shown in Fig. 1, a piezo-electric accelerometer measured axial acceleration and a strain-gage mea-

Table 2 Description of the drilling system

Spiral Drill Collars:

$$6.5 \text{in OD} \times 2\frac{13}{16} \text{in ID} \times 30.5 \text{ ft}$$

80.4 lb/ft in Air

Aluminum Pipe with steel tool joints:

4.6in OD$\times 3.6$in ID$\times 30.2$ft

10.75lb/ft with tool joints in Air

Elongation	0.0133ft for 1000ft long pipe with with 1Klb tensile force
Pipe Body	4.6in OD over 21 ft length, thickening at both ends to 5.031 in OD for 7 in length at 0.107in/ft rate of taper
Tool Joints	$6\frac{1}{8}$in OD$\times 5.031$ in ID$\times 10$ in

Hoisting System:

Blocks	18.62slugs
Power Swivel	99.38slugs
Wire Rope	K(spring constant)=200Klb/ft

Formation: dolomite

Bit: 8.5in F-5 tricone insert bit

Drilling Mud: 9.13lb/gal

Table 3 Material properties

Steel:	Density=15.18slug/ft³ Young's Mod.=4.321×10^9lb/ft²
Aluminum:	Density=5.428slug/ft³ Young's Mod.=1.531×10^9lb/ft²
Mud:	Density=2.027slug/ft³ Viscosity=2.1×10^{-4}lb sec/ft²

sured axial force, at the power swivel The notations used in this paper are as shown below:

F_s : Force at the swivel

A_s : Acceleration at the swivel

3. Theoretical Analysis

The transfer function between the measured force and acceleration at the swivel is a measure of the drive point impedance of the system below the measurement point. Fig. 2 shows the analytical model to predict the drive point impedance. Since the strain-gage is located between the swivel and a frame which is connected to the cables, then the top element of the model must represent the 99.38 slug swivel mass. The drillstring is modelled as an equivalent stepwise uniform bar and the bottom boundary condition is modelled by an equivalent spring and damper.

To predict the transfer functions for the axial vibration model in Fig. 2, a computer code has been implemented as explained in Section 1.

3.1 Equivalent Uniform Bar

A drillstring is assembled from sections of pipe approximately 30 ft in length. The ends of each section have threaded tool joints with cross-sectional
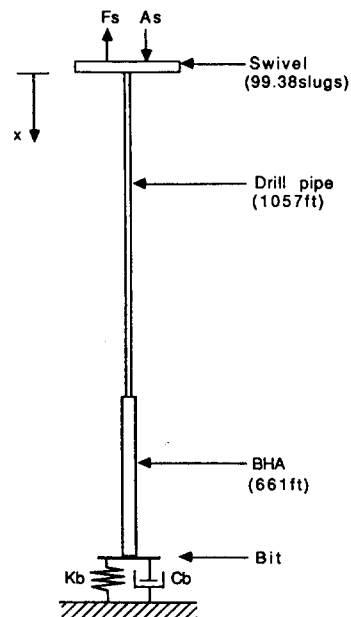

Fig. 2 Analytical model for topside excitation tests

areas that are several times larger than the pipe body, as shown in Fig. 1. However, if the frequency of interest is so low that its wavelength is long compared to the spacing of the tool joints, the pipe can be modelled as a one equivalent uniform bar, which has the same mass and the same elongation per unit applied force.

In this analysis, the drill pipe is modelled as an equivalent uniform bar and the BHA is modelled as another equivalent uniform bar, from the data in Table 2 and Table 3. The results are in Table 4. In this table, ρ_e, E_e, A_e, c_e, and l denote in order the density, Young's modulus, cross-sectional area, axial wave propagation speed, and length of each equivalent uniform bar.

3.2 Effect of Mud

The effect of mud viscosity on the drillstring axial vibration is estimated as an added mass(m') and damping(c_m) distributed along the drillstring, and can be expressed as follow[9] :

$$m' = 2\pi(a+b)\sqrt{\frac{\rho_m\mu}{2\omega}} \qquad (1)$$

$$c_m = 2\pi(a+b)\sqrt{\frac{\rho_m\mu\omega}{2}} \qquad (2)$$

where

ρ_m, μ : Density, viscosity of mud
a, b : Inner, outer radius of drillstring

ω : Circular frequency

Therefore, the equation governing the axial motion of the drillstring becomes :

$$(\rho_e A_e + m')\frac{\partial^2 u}{\partial t^2} + c\frac{\partial u}{\partial t} = E_e A_e \frac{\partial^2 u}{\partial x^2} \qquad (3)$$

u : Axial displacement
x, t : Axial coordinate, time coordinate
c : Damping coefficient per unit length

The damping due to the mud viscosity is included in c, and is given with other dampings in Table 5.

3.3 Damping

Damping of drillstrings comes from following potential sources[1~3]; losses due to the motion of the drillstring in the viscous drilling fluid(c_m), radiation losses into the surrounding formation(c_r), internal losses in the tool joints and the drillstring, and frictional losses due to rubbing against the wall. Damping from the bottom boundary is discussed in the bottom boundary condition in the following subsection.

If the axial wave propagation speed in the drillstring is faster than the shear wave propagation speed in the surrounding formation, waves radiate radially into the formation. This radiation damping(c_r) can be obtained from reference[9]. And the mud viscous damping(c_m) can be obtained from Equation (2), The

Table 4 Equivalent uniform bars for drill pipe and BHA

	ρ_e[slug/ft³]	E_e[lb/ft²]	A_e[ft²]	c_e[ft/sec]	l[ft]
Drill Pipe	5.428	1.222×10^9	0.06151	15004	1057
BHA	15.18	4.314×10^9	0.1645	16858	661

Table 5 Damping coefficients[$lb\ sec/ft^2$]

	Drill pipe			BHA		
	c_m	c_r	c_0	c_m	c_r	c_0
WOB= 0Klb	$0.078\sqrt{f}$	$1.85\times10^{-9}f^3$	0.25	$0.089\sqrt{f}$	$1.09\times10^{-8}f^3$	0.25
WOB=10Klb	$0.078\sqrt{f}$	$1.85\times10^{-9}f^3$	0.5	$0.089\sqrt{f}$	$1.09\times10^{-8}f^3$	0.5
WOB=20Klb	$0.078\sqrt{f}$	$1.85\times10^{-9}f^3$	0.8	$0.089\sqrt{f}$	$1.09\times10^{-8}f^3$	0.8
WOB=30Klb	$0.078\sqrt{f}$	$1.85\times10^{-9}f^3$	1.2	$0.089\sqrt{f}$	$1.09\times10^{-8}f^3$	1.2

(where f is frequency in hertz)

damping due to other effects have been lumped together, and have been determined from the experiments so as to provide a good match in the amplitudes of the predicted and measured transfer function at the swivel. In this research, this damping coefficient(c_o) is modelled as being dependent on WOB but not on frequency. The damping coeffcient(c) in Equation (3) can therefore be expressed as the sum of the individual contributions:

$$c = c_m + c_r + c_o \tag{4}$$

Estimates of the damping for the drillstring in the field experiments are listed in Table 5. The radiation damping in Table 5 is estimated by assuming that the surrounding formation is clay. The radiation damping is relatively small compared to other dampings, in the frequency range of this research. However, this radiation damping increases as frequency increases and may become dominant, because it is proportional to the cube of the frequency.

3.4 Bottom Boundary Condition

The bottom boundary condition depends on the nature of the contact between the bit and the formation. The introduction of a model of the bottom boundary condition is one of the features of approach taken in this research which distinguishes it from prior work. Existing models predict the critical rotational speed or the resonance of the drillstring by neglecting the flexibility of the bottom formation.

As long as the bit stays in contact with the bottom formation, the bottom boundary condition of drillstring can be approximately modelled by an equivalent spring-damper system which simulates the bottom formation, as shown in Fig. 2. The evaluation of this bottom boundary condition model is one of the principal contributions of this research. It is simulated as a free boundary for when the bit is off the bottom. At various WOB's without rotation, the spring constant(K_b) and the damping coefficient(C_b) are chosen to give approximately the same resonant peak frequencies in the predicted as well as measured transfer functions. The values assigned for the spring and damping coeffcients for the bottom

Table 6 Bottom boundary conditions for each WOB

	K_b[lb/ft]	C_b[lb sec/ft]
WOB= 0Klb	0	0
WOB=10Klb	1×10^7	1×10^4
WOB=20Klb	1×10^8	1×10^4
WOB=30Klb	5×10^8	1×10^4

boundary condition model are WOB dependent and are listed in Table 6.

4. Experimental Results and Comparisons with Analytical Results

4.1 Off-Bottom Test

The force and acceleration at the swivel were measured during the topside excitation, when the bit was off the bottom. The measurements were taken at various RPM's(0,30,60,84)to investigate the effect of RPM on the drillstring axial vibration. Only the results at 30 RPM are presented in this paper, because the measured results are invariant with respect to the RPM change and the best coherence was obtained at this RPM.

Fig. 3(a) and Fig. 4(a) show the magnitude and phase of the measured acceleration per unit force transfer functions, A_s/F_s, with solid lines. The principal features of Fig. 3(a) are 4 peaks at 2.95, 8.75, 12.5, and 15.5 to 16.5 Hz as well as 3 zeros at around 7, 12, and 14.65 Hz. Also, the phase plot of the transfer function reveals shifts of plus π radians around each of these zero frequencies and minus π radians around each of these peak frequencies, as shown in Fig. 4(a). The shift of minus π radians around 0 Hz represents a mode with rigid body motion. The peak at 0 Hz can not be seen in the magnitude of the transfer function because acceleration can not have a peak at 0 Hz.

In these figures, dashed lines show the magnitude and phase of the predicted transfer function based on the analytical model in Section 3. A free boundary condition is assumed at the bit because the bit is off the bottom(K_b=0, C_b=0). The damping of the drillstring is chosen to provide a good match in the amplitudes of the predicted transfer function and the
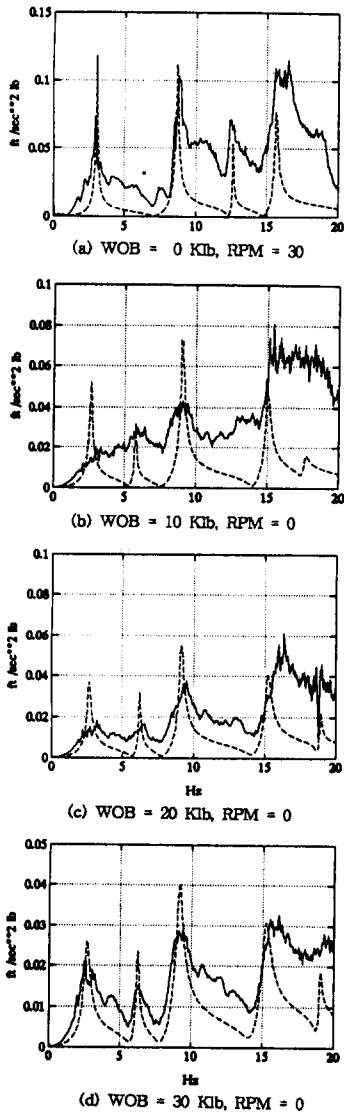
Fig. 3 Magnitudes of measured (solid line) and predicted (dashed line) transfer functions
(Freq. Resol.=0.05 Hz, No. of Averages=16)

Fig. 4 Phases of measured (solid line) and predicted (dashed line) transfer functions
(Freq. Resol.=0.05 Hz, No. of Averages=16)

measured one. The predicted transfer function has the similar resonant peak frequencies and zero frequencies as the measured one, and the predicted phase plot is also in good agreement with the measured one.

The mode shapes at each resonant peak frequency in the predicted transfer function are as shown in Fig. 5. The predicted modes at 3.05, 8.65, and 15.65 Hz are called pipe modes because they have large motion in the drill pipe and small motion in the
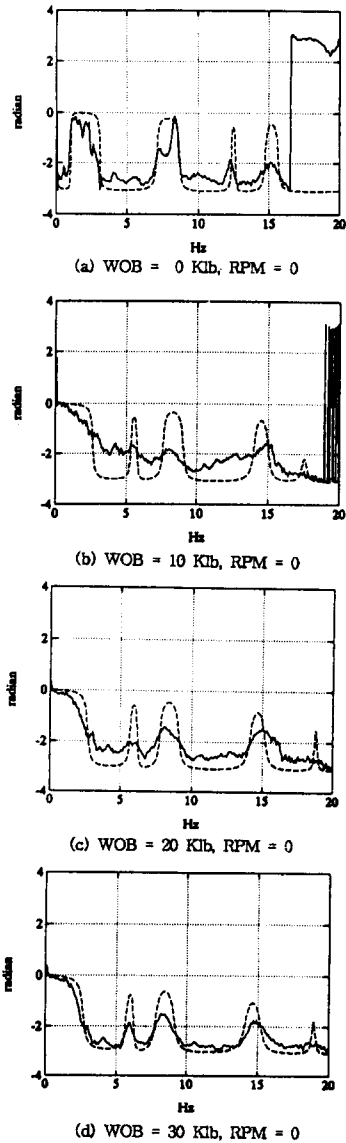
BHA. The mode at 12.6 Hz is called a BHA mode or a global mode, since it has large motion also in the BHA. The pipe modes are insensitive to the bottom boundary condition due to the small motion in the BHA, whereas BHA modes are sensitive to the bottom boundary condition, as will be demonstrated in the following subsection.

The good agreement between the measured and predicted results gives considerable confidence to the use of the analytical model proposed in Section.
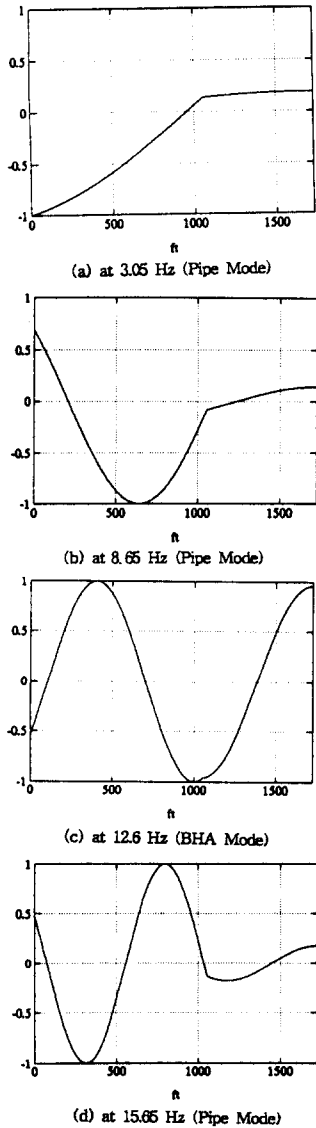
(a) at 3.05 Hz (Pipe Mode)

(b) at 8.65 Hz (Pipe Mode)

(c) at 12.6 Hz (BHA Mode)

(d) at 15.65 Hz (Pipe Mode)

Fig. 5 Predicted displacement mode shapes with free bottom boundary condition
(Topside is to the left)

3. These tests also revealed that the dynamic properties of the drillstring axial vibration were RPM independent. However, the excitation at the bit would be RPM dependent when drilling.

4.2 On-Bottom Test without Rotation

To investigate the effect of the WOB on the effective bottom boundary condition, the force and acceleration at the swivel were measured during topside excitation at 3 different WOB's(10, 20, 30

Klb) without rotation. In Fig. 3 and Fig. 4, solid lines show the magnitudes and phases of measured acceleration per unit force transfer function(A_s/F_s), and dashed lines show the magnitudes and phases of the predicted transfer functions based on the analytical model in Section 3.

For each WOB, the bottom boundary condition used in the prediction is chosen to provide a good match in the peak frequencies of the predicted and measured transfer function, and is given in Table 6. As WOB increases, the apparent spring constant of the bottom increases and approaches a fixed condition. The distributed dampings of the drillstring are also chosen to provide a good match in the amplitudes of the predicted and measured transfer functions, and These are given in Table 5.

Fig. 6 shows the mode shapes at the peak frequencies in the predicted transfer function for 30 Klb WOB. The peaks at 6.25 and 19.05 Hz are due to BHA modes, and the others are due to pipe modes. As bottom stiffness increases, the resonant frequencies of the BHA modes increase; thus, the resonant frequencies of the BHA modes with a free bottom boundary condition at 0 Hz and 12.6 Hz in the previous subsection, move up to 6.25 Hz and 19. 05 Hz with the more rigid boundary condition appropriate for 30 Klb WOB. The resonant frequencies of the BHA modes for 0 WOB at 0 HZ and 12.6 Hz are close to the resonant frequencies of the BHA with a free-free boundary condition, and those for 30 Klb WOB at 6.25 Hz and 19.05 Hz are close to the resonant frequencies of the BHA with a free-fix boundary condition.

In contrast to these BHA modes, the pipe modes are relatively insensitive to the bottom boundary condition or WOB, because they have small motion at the bit. As WOB increases from 0 to 30 Klb, the resonant frequencies of the pipe modes do not change significantly, 3.05 Hz, 8.65 Hz, and 15.65 Hz to 2.65 Hz, 9.15 Hz, and 15.25 Hz. Also, the mode shapes do not show significant differences, as shown in Fig. 5 and Fig. 6.

An important conclusion of these tests is that the bottom boundary condition depends on the WOB as shown in Table 6 for non-drilling conditions, and the
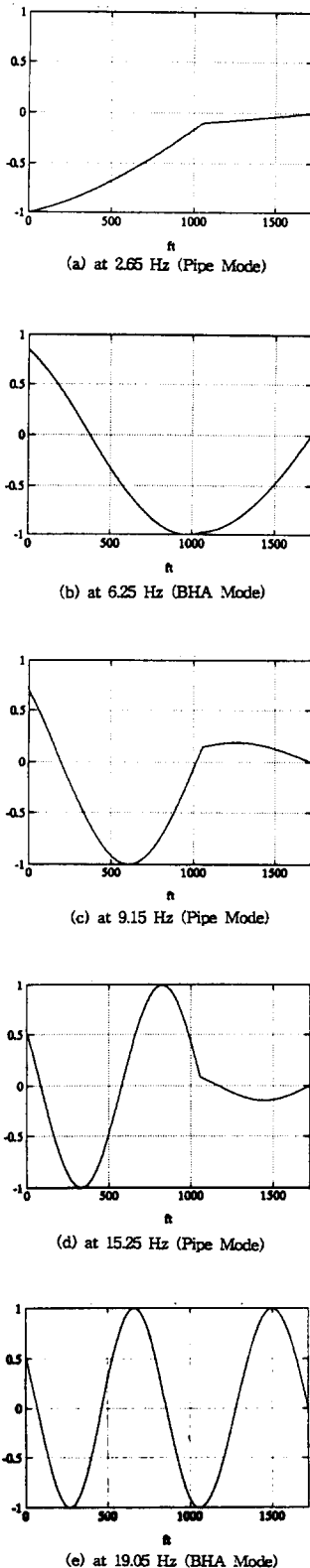
(a) at 2.65 Hz (Pipe Mode)

(b) at 6.25 Hz (BHA Mode)

(c) at 9.15 Hz (Pipe Mode)

(d) at 15.25 Hz (Pipe Mode)

(e) at 19.05 Hz (BHA Mode)

Fig. 6 Predicted displacement mode shapes for 30 Klb WOB

(Topside is to the left)

pipe modes are insensitive to the bottom boundary condition but the BHA modes are not.

5. CONCLUSION

In this paper, the axial vibration properties of a typical drillstring were studied. The drillstring was modelled as an equivalent stepwise uniform bar with spring-damper bottom boundary condition. The mechanical properties of the equivalent uniform bars and the effect of the surrounding layers, such as the mud and formation, are evaluated theoretically. A forced vibration testing technique was developed, which utilized the hydraulic ram as a source of oscillatory axial excitation, to experimentally evaluate the damping and the bottom boundary condition.

The good agreement between measured results of the off-bottom test and predicted results for the drillstring with a free boundary condition, gives considerable confidence to the use of the analytical model proposed in Section 3. This test also revealed that the dynamic properties of drillstring axial vibration are RPM independent.

The on-bottom test without rotation shows that the bottom boundary condition strongly depends on the static WOB. An important conclusion of this test is that the flexibility of the rock must be included to predict the resonant frequencies of the drillstring axial vibration.

The effective bottom boundary condition while drilling would be quite different than under weighted but non-rotating conditions. The difference is that while rotating, the bit is fracturing the rock. This would introduce a lower equivalent stiffiness at rock-bit boundary and introduces additional damping. However, it will strongly depend on the static WOB also.

References

(1) Angona, F.A., 1965, "Drill String Vibration Attenuation and Its Effect on a Surface Oscillator Drilling System", Journal of Engineering for Industry, ASME, pp. 110~114.

(2) Dareing, D.W. and Livesay, B. J., 1968, "Longitu-

dinal and Angular Drill String Vibration with Damping", Journal of Engineering for Industry, pp. 671~679.

(3) Squire, W.D. and Whitehouse, H.J., 1979, "A New Approach to Drill-String Acoustic Telemetry", SPE Conference Paper Number 8340, September.

(4) Dareing, D.W., 1984, "Guidelines for Controlling Drill String Vibrations", Journal of Energy Resources of Technology, ASME, pp. 272~277.

(5) Aarrestad, T.V. and Tennesen, H. A. and Kyllingstad, A., 1986, "Drill String Vibrations: Comparison Between Theory and Experiments on a Full-Scale Research Drilling Rig", Proceedings of LADC/SPE Conference.

(6) Clayer, F., Vandiver, J. K., and Lee, H.Y.Lee, 1990, "The Effect of Surface and Downhole Boundary Conditions on the Vibration of Drillstrings", SPE Conference Paper Number 20447.

(7) Thomson, W.T., 1972, Theory of Vibration, Prentice-Hall, Inc., pp. 219~221, 242~245.

(8) Meirovitch, L., 1967, Analytical Methods in Vibrations, pp. 76~81, 251~257.

(9) Lee, H.Y., 1991, Drillstring Axial Vibration and Wave Propagation in Boreholes, PhD thesis, Massachusetts Institute of Technology.